AGH UNIVERSITY OF SCIENCE AND TECHNOLOGY

Faculty of Material Science and Ceramics

Department of Ceramics and Refractories

A PhD DISSERTATION

Inconel 625 – Tungsten Carbide Composite System for Laser Additive Manufacturing

Jan Huebner

Supervisor

Prof. dr hab. inż. Dariusz Kata

KRAKÓW, POLAND

2020

AUTOREFERAT

Table of contents

AUTOREFERAT 2
Table of contents 2
1. Background 3
2. Research objectives 3
3. Motivation 4
4. Laser additive manufacturing of Inconel 625 – WC MMC 6
5. Experimental procedure 11
6. Laser cladding of Inconel 625 – WC (D_{WC_1} = 0,64 μm) 11
7. Laser cladding of Inconel 625 – WC (D_{WC_4} = 6,13 μm) 19
8. Heating rate effect on microstructure of Inconel 625 – WC system 24
Conclusions 27
Bibliography 28

1. Background

The need for innovation in industry leads to constant evolution of materials and their production methods. Last fifteen years, showed that individual design and ability to adapt for new challenges are the major driving forces in material science. The possibilities presented by rapid development of specialized equipment offer solutions for problems that were unsolvable few years ago. The invention of additive manufacturing methods, sometimes called 3D printing – changed the world. Something that was perceived as technological curiosity, very quickly became global trend with enormous market.

The new method of production for mostly polymer – based prototypes, rapidly evolved into all branches of industry. Nowadays, so called 3D printers can be easily found in both homes and huge factories. Because of additive manufacturing popularity, materials that we already know, need to be investigated for their suitability for 3D printing.

Ni – based alloys are commonly used in aerospace and power industries. Because of good corrosion resistance combined with weldability and ability to be modified by addition of different phases, they can be potentially used in additive manufacturing. Lasers are excellent as energy source for metals deposition because of their higher melting point than polymers. Laser cladding is a method that uses energy delivered to material in form of laser beam in order to melt and solidify new structures, It allows for superior control of process parameters which results in very small interference in substrate together with good quality of obtained coating.

Nowadays, power industry strives for innovations that could allow more efficient way of electricity production. Materials that can withstand both high temperature and chemically aggressive environments have potential to be used in turbine engines [1–3]. The easiest way to improve effectiveness of gas turbines is to increase work temperature. The blades are constantly exposed to chemical and mechanical factors which result in damaged material surface. It begins with appearance of microcavities and proceed to irreversible changes of material microstructure due to prolonged exposure to aggressive environment. Because there is no reliable and cost efficient technique of material regeneration, laser cladding of Ni – based Metal Matrix Composite was proposed and investigated in this dissertation. In order to check its potential as material for additive manufacturing, Inconel 625 – WC composite system was subjected to series of experiments,

2. Research objectives

In this dissertation Metal Matrix Composite (MMC) with ceramic reinforcement in form of tungsten carbide (WC) was proposed as a material suitable for laser cladding. Usually, aggressive environment and long exposition to elevated temperatures may result in relatively short lifespan of materials used as blade turbines, boiler coatings etc. The opportunity to regenerate damaged element is economically attractive. However, conventional welding techniques such as Metal Inert Gas (MIG) or Tungsten Inert Gas (TIG), are dangerous because of large amount of heat delivered to the substrate. This leads

to microstructure and phase composition changes of substrate material. In order to prevent interference within the substrate, laser cladding was proposed and investigated as potential solution. The energy delivered to material in form of laser beam causes precise heating of small area of material and then is followed by rapid cooling. Due to high processing speed, obtained microstructure is refined in comparison to conventional methods. Superior control of process parameter allows designing of material properties.

Inclusion of WC particles in Ni – based metal matrix was expected to induce microstructure changes and improvement of material hardness. However, due to chemical complexity of the system, it is hard to predict its behavior during high intensity laser processing. Because of that, thorough analysis and evaluation was needed in order to properly describe how processing of Inconel 625 – WC system changes its properties.

At the beginning, deposition of pure Inconel 625 coating was investigated in order to check material suitability for laser cladding. Then, experiment proceeded to next step which was introduction of WC particles as reinforcement into the Ni – based alloy matrix. The initial research objective was to obtain MMC with uniform distribution of WC in whole volume of the material. Optimization of process parameters and selection of powders were main factors that affect quality of obtained material. Fine WC (D_{WC1} = 0,64 μm) powder was used to prepare mixtures with different weight ratio of Inconel 625 and WC. However, due to high temperatures reached during processing, carbide particles dissolved in Ni – based matrix. This leads to next step, in which fine WC powder was replaced with other WC powder (D_{WC4} = 6,13 μm) in mixtures. Deposition of modified material showed, that it is possible to prevent complete dissolution of WC particles. In order to better understand composite behavior, Differential Thermal Analysis (DTA) was performed on powder mixtures containing two WC powders. Samples obtained with varying heating conditions and WC weight content were microstructurally examined by means of Scanning Electron Microscopy (SEM). It allowed observation of microstructure evolution in Inconel 625 – WC system. Finally, deposition of material with high content of WC was investigated under low <500 W and high >1000 W power by using lasers with disc and CO_2 laser beam sources. The examination of all prepared samples provided data that allowed to describe the material transformation during laser cladding process.

Results obtained from conducted experiments answered important question:
“Is Inconel 625 – WC composite system suitable for laser additive manufacturing?”

3. Motivation

Application of gas turbines for energy production is increasing year – by – year. Low emission of exhaust gases, relatively small sizes and ability to quick start-up are their main advantages. The rising need for clean and cheap energy made big companies like ABB, Siemens and Westinghouse invest in development of more efficient devices that can work at high temperature. Improvement from 1000 – 1150°C to 1200 – 1400°C resulted in rise of engine efficiency from 35 – 40% to 50 – 60%. It can be improved even further by rising average temperature at inlet source of heat for open turbines. For closed turbine

engines there is a possibility to decrease average temperature by internal cooling channels but it is costly due to its complexity and manufacturing difficulties.

Easiest solution lays in design of the material that is suitable for prolonged work at both aggressive environment and elevated temperature. The rotor blades, steering blades and discs are gas turbine parts that work at the highest temperature [4]. The requirements for the components working under such conditions includes good creep resistance and excellent tribological properties. Nowadays, two methods can be used for mass production of turbine blades:

1) Blades cooled by air flow through internal cooling channels system – because of geometrical complexity and precision needed to produce such piece, production cost is very high and often unprofitable. Internal channels are responsible for higher failure rate of parts produced by this method – Fig. 2.1a.
2) Protective coatings characterized by improved high temperature properties, at critical parts of blade. This method is efficient and cheaper in comparison to internal cooling channels – Fig. 1b.

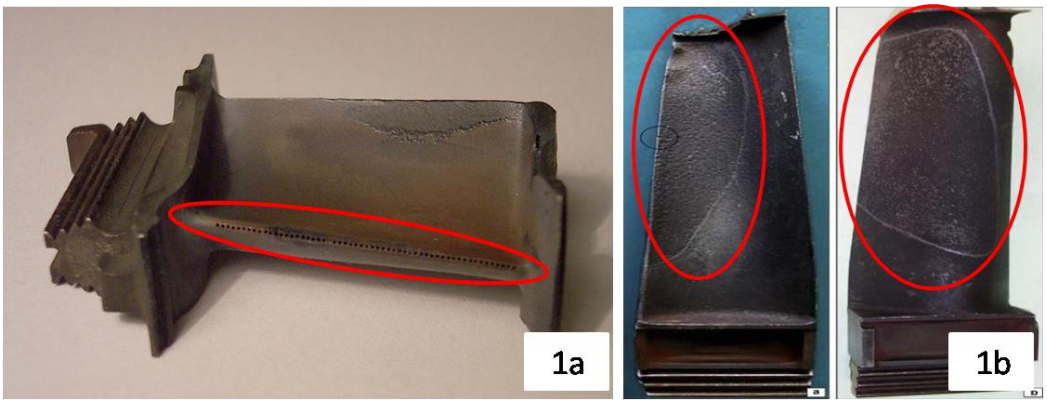

Fig. 1. *Turbine blades: a) cooling canals inside the blade; b) protective coating on blade surface*

Because of challenging geometry of manufactured parts, most of conventional methods of MMCs manufacturing cannot be used. Additionally, due to chemically complex composite systems, need for rapid, reliable and repeatable technique is required to ensure quality of fabricated material. Because of that, additive manufacturing (AM) method of Laser Engineered Net Shaping (LENS) also called Laser Cladding (LC) is often used to obtain superalloys coatings such as: Stellite 6, 12, 21, 156, 157, 158, Inconel 625, 718, 738, 800H [5–9]. These materials are suitable for work under high tension in temperature close to their melting points. They possess excellent corrosion resistance and are stable with increasing work temperature.

The technology chosen for coating deposition have huge impact on properties of wear and corrosion resistant coatings. Surface layers produced from the same material but with different techniques have varying physical and performance properties. Depending on the used methods, differences can be significant. Most common industry

scale production methods of metal and ceramic coatings are thermal spraying [10,11] plasma arc welding and laser cladding [10,12,13].

In this work, Metal Matrix Properties (MMC) on an example of Inconel 625 – WC system is discussed. Due to rapid processing of composite system and its non – equilibrium state after solidification, obtained material exhibits formation of phases that usually appear after extensive heat treatment. Introduction of W and C in form of tungsten carbide induces different behavior of alloy 625 due to enhanced element microsegregation in material.

4. Laser additive manufacturing of Inconel 625 – WC MMC

Nowadays, Ni – based alloys are widely used for many specialized applications in aircraft, power, transportation, defense and petrochemical industries. Thanks to their properties such as excellent weldability, ductility and toughness at low temperatures, good corrosion resistance, high strength and stability at elevated temperatures, they fit well in different working conditions.

There is no strict classification system that contain all of different Ni – based alloys. They are mostly divided by composition as shown in Fig. 2. [14].

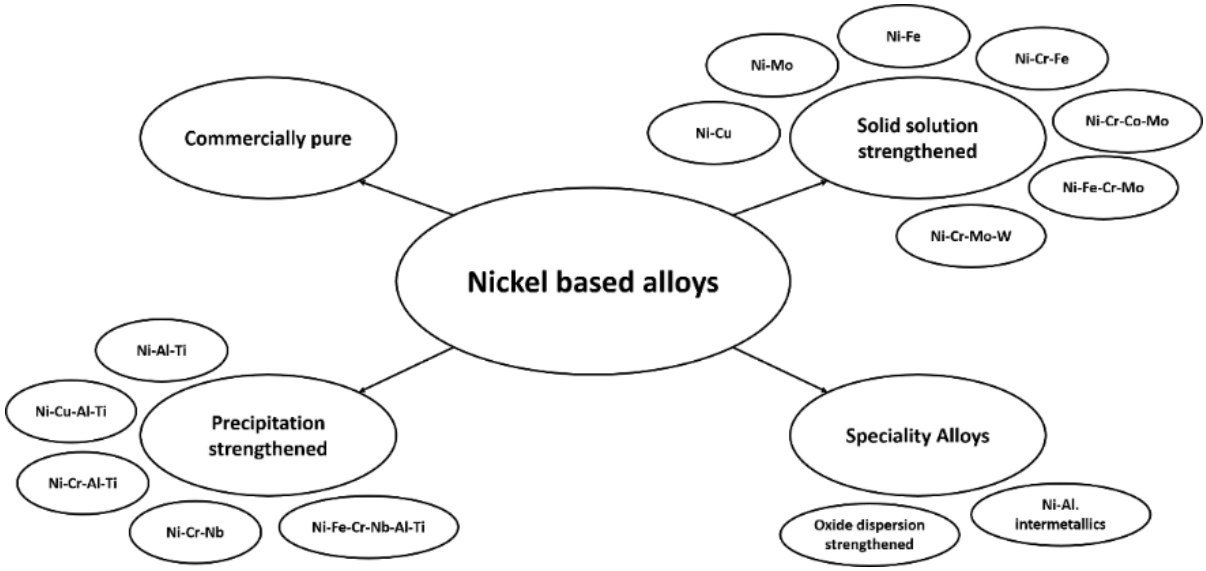

Fig. 2. *Classification of Ni – based alloys based on composition* [14]

In order to enhance specific properties of alloy, WC was chosen as reinforcement material. It is characterized by excellent wettability by liquid Ni, which guarantees good connection between both phases after laser processing. However, due to increased reactivity on the WC – Inconel 625 boundary, formation of secondary phases containing alloying elements is possible. It is further enhanced by element segregation during rapid solidification of composite material.

Elements like Al, Ti, Mn, Nb, Mo and W are characterized by adequate size ratio of maximum about ± 0,17 in comparison to Ni. They also exhibit acceptable solubility in Ni

in 1000°C. Combination of these two properties allows for solid solution strengthening. If Cr or Mo are present, long term exposition to elevated temperature promotes solid state precipitation reactions. This leads to eutectic – like reactions that occurs at the end of solidification, thus formation of Cr and Mo rich secondary phases is possible.

Laser Engineered Net Shaping (LENS) is the most advanced of presented methods. It is characterized as directed energy deposition and is also known as 3D Laser Cladding, Directed Metal Deposition (DMD), Directed Light Fabrication (DLF), Laser – Based Metal Deposition (LBMD), Laser Freeform Fabrication (LFF) and others [15–17]. In this method powder or wire material is delivered under the laser beam in order to obtain molten pool. As the laser head moves forward in previously designed way, melted material solidifies and forms singular layer as it is shown in Fig. 3.

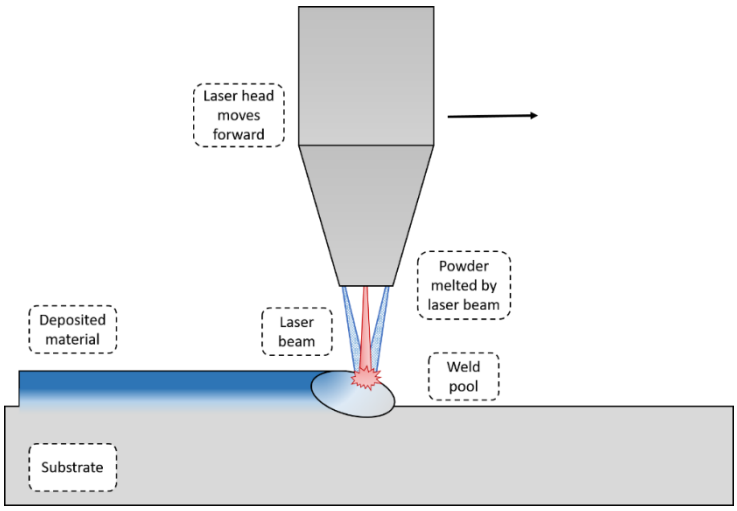

Fig. 3. *Schematic representation of LENS apparatus*

As the energy is delivered to surface in form of laser beam, the heat is distributed thorough the material as shown in Fig. 4. In order to reduce energy loss and improve melting efficiency of powders, bulk absorption coefficient (β) was introduced [20]. It gives the information about the particular component of energy to total supplied energy ratio. Both, energy balance and corresponding bulk absorption coefficient are described by equations (1) and (2) respectively [20]. It was confirmed that generally laser cladding has about 40-45% energy efficiency [20].

$$Q_{in} = Q_{ABS} + Q_{DEP} + Q_{REF} + Q_{LOST} \quad (1)$$

$$\beta_{ABS} + \beta_{DEP} + \beta_{REF} + \beta_{LOST} = 1 \quad (2)$$

where:
Q_{ABS} (β_{ABS}) – energy absorbed by substrate
Q_{DEP} (β_{DEP}) – energy absorbed by powder
Q_{REF} (β_{REF}) – energy reflected by substrate
Q_{LOST} (β_{LOST}) – energy lost by powder due to lack of fusion and evaporation

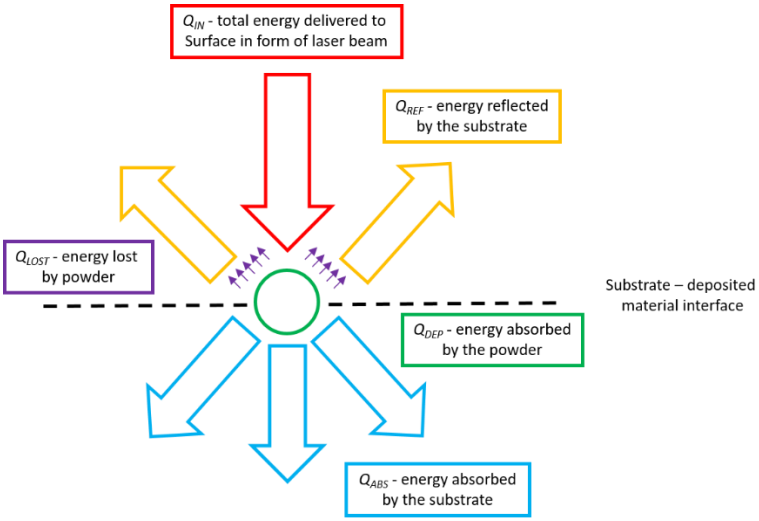

Fig. 4. *Laser beam – material surface interaction*

The laser cladding technique is suitable for processing of Ni – based alloys with carbide reinforcement due to operation wavelength of commonly used Nd:YAG and Yb – fiber lasers. Because of the introduction of ceramic reinforcement, it is necessary to use laser beam source that is characterized by good absorptivity by both materials. However, to achieve desired strengthening effect, process parameters should be optimized in a way that allows for metal melting and preservation of original morphology of ceramic particles. Microstructure of laser cladded materials are affected by different parameters as shown in Fig. 5.

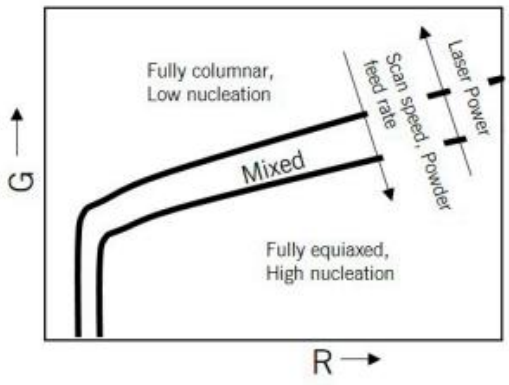

Fig. 5. *Columnar to equiaxial transition (CET) trend in relation to G and R* [21]

Inconel 625, is a Ni – Cr – Mo – Nb alloy is able to form secondary phases due to high content of Nb, Si and C [22–24]. The addition of those elements increased melting point of alloy. Because of Nb presence, solidification terminates with formation of γ – Ni and Nb rich phases of NbC and Laves as a result of eutectic like reactions. The addition of carbon to the system, promotes appearance of NbC [25,26]. Thanks to good wear and corrosion resistance [27], Inconel 625 is extensively used as protective coating of carbon steels and Cr – Mo components.

Formation of Cr, Mo, Nb and W carbides is dependent on temperature in which reaction occurs. It can be observed that formation of $Cr_{23}C_6$ is promoted in whole temperature range up to 2000 K. It is followed by Cr_7C_3 which free enthalpy ΔG is even lower in higher temperatures. Formation of NbC is generally stable in whole temperature range. Cr_2C_3 and Nb_2C exhibits similar ΔG values in lower temperatures which become more diverse during heating. W and Mo carbides are the least favorable to obtain as presented below [28,29,38,39,30–37].

Because of phase and elemental complexity of proposed composite, the behavior during laser cladding of the Inconel 625 – WC system is hard to predict. Some research concerning introduction of coarse carbide particles (D_{WC} > 10 μm) into Inconel 625 matrix were reported [40,41]. However, due to size of the carbide particles, fabricated structures were not homogenous as it is presented in Fig. 6 [41]. As a result, the properties of material can differ depending on measured area. It was observed that, coarse WC particles partially dissolved at grain/matrix region which induced formation of fine precipitates.

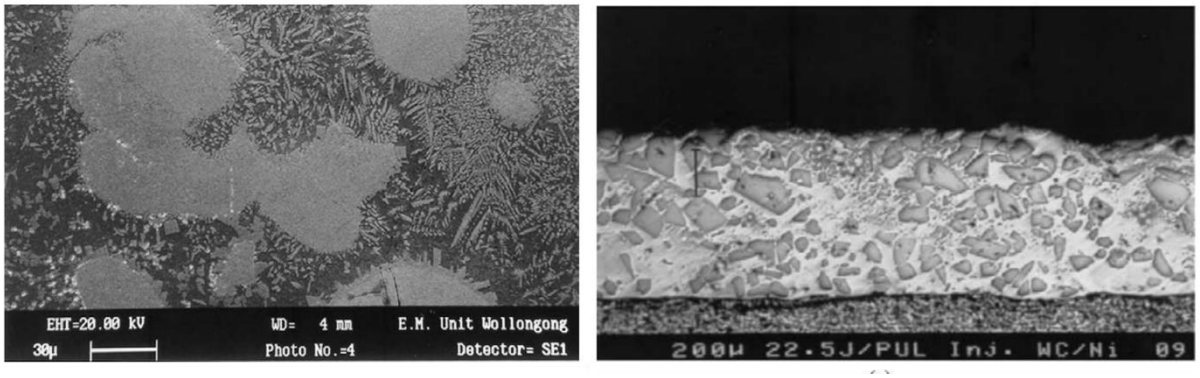

Fig. 6. *Non uniform distribution of coarse WC throughout the material* [41]

Dissolution of reinforcement ceramic particles was widely reported by different authors [42–51]. Because of good wettability of commonly introduced carbides, Ni – based alloys tend to dissolve them in higher temperatures between 750°C – 950°C [43,51,52]. Boundary between carbide particle and metal acts as interlayer enriched in Cr, Mo and Nb – Fig. 7 [46]. As a consequence depletion of these alloying elements in matrix was observed [46,50–54]. Different Ni – based alloys exhibited formation of secondary carbides together with TCP phases (Laves, δ, η) [45,46,48–52,54–56]. Due to aggressive microsegregation of Mo, Nb and to lesser extent Cr, solidification of secondary phases can occurr by eutectic – like reaction at the end of solidification [48,49,54,56].

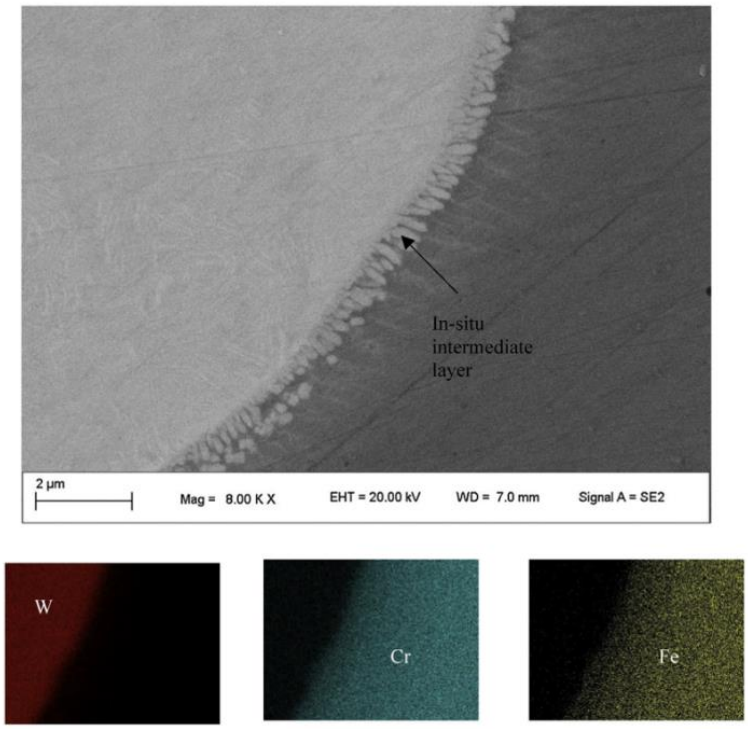

Fig. 7. *Partial dissolution of WC in Inconel 625 laser cladded composite* [46]

5. Experimental procedure

The experimental procedure was divided into four parts. Each of them focuses on different aspect of laser deposition of Inconel 625 alloy or Inconel 625 –WC system.

- **Part I** – in which laser cladding of Inconel 625 alloy on steel substrate was described.
- **Part II** – describes preparation route of Inconel 625 – WC metal matrix composites which contains up to 30 wt % of WC.
- **Part III** – in which microstructural evolution of Inconel 625 – WC system was investigated by heating powder mixtures in varying conditions.
- **Part IV** – based on results from parts I, II and III, laser cladding of Inconel 625 – WC 30 wt % composite material was performed by CO_2 and disc laser apparatus.

6. Laser cladding of Inconel 625 – WC (D_{WC_1} = 0,64 µm)

In order to prepare Inconel 625 – WC powder mixtures, Castolin Eutectic EuTroLoy 16625 metallic powder with composition shown in Table 1 and average diameter of d_{Inc} ≈ 104 µm was used together with WC_1 powder with average diameter of D_{WC_1} = 0,64 µm.

To prepare 100 g of powder mixture, weighted amount of powders were put inside isolated milling chamber. Homogenization of mixture was done with addition of isopropyl alcohol, using cemented carbides grinding media in weight ratio 1:1 to powders. Homogenization process lasted for 90 minutes and was followed by drying of powders in 80°C for 6 hours. Morphology of obtained mixtures were examined by SEM equipped with EDS detector. As seen in Fig. 8, there was no satisfactory adhesion between metal and ceramic particles after initial homogenization.. Therefore, addition of binder was needed. Because of already high content of carbon introduced to system, two carbon based organic binders were proposed in form of epoxy resin and dextrin. The XRD phase analysis showed presence of Ni and WC in powders.

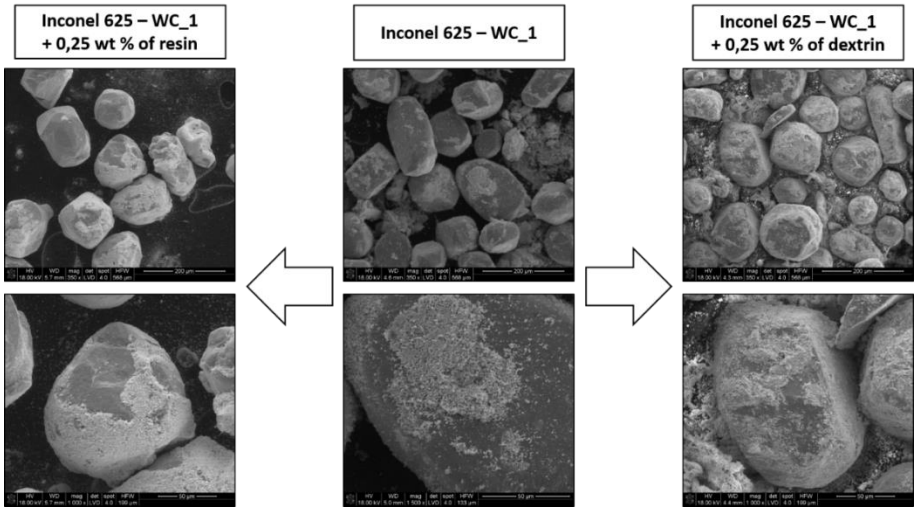

Fig. 8. *Powder mixtures with 0,25% wt % resin (left) and 0,25 wt % dextrin (right) after 90 min of homogenization*

Table 1. *Compositions of powder mixtures made with WC_1 powder*

Powder mixture	Inconel 625 [wt %]	WC [wt %]	Carbon content [wt %]
Inc_WC10_0_64	90	10	0,61
Inc_WC20_0_64	80	20	1,22
Inc_WC30_0_64	70	30	1,83

Laser cladding of Inconel 625 – WC composite system was performed using modular laser apparatus JK2000FL of JK Laser Company. It was equipped with Yb – doped fiber laser beam source with wavelength of 1063 ± 10 nm suitable for processing of both Inconel 625 and WC powders.

The schematic of laser set-up is shown in Fig. 9. Laser cladding process starts with powder mixture transport from powder feeder to laser head by external tube. Powder is carried by inert Ar inert gas in order to avoid surface oxidation. Then, it is sprayed onto substrate by 4 nozzles located around optics of laser head. Modular laser beam source provides high intensity electromagnetic radiation by combining power of 3 laser source modules into one. Laser beam is then transferred to laser head by high quality Yb doped fiber. Powder grains are melted by laser beam and then mixed with substrate. Formation of melt pool is observed in area affected by laser beam. Inconel 625 – WC/substrate melt is then rapidly cooled and solidified as laser head moves forward which results in formation of first layer of coating. Simultaneously inert gas is supplied directly to laser head in order to shield optics from powders. Laser source needs to be constantly cooled down by external water cooling system during whole process due to high temperature of modules.

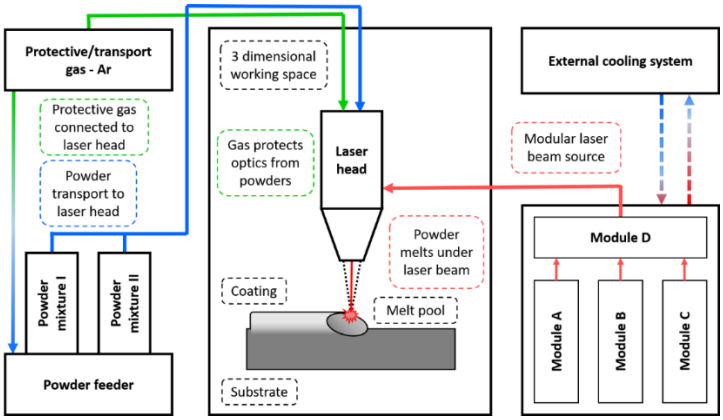

Fig. 9. *Schematic representation of JK2000FL laser apparatus for deposition of Inconel 625 – WC system*

Temperature measurements were conducted by radiation pyrometer during laser processing for laser power of 320 W as shown in Fig. 10. Obtained data is presented in

Fig. 11. Laser power used during process was sufficient for melting of Inconel 625 (melting point $T_{Inc} \approx 1340°C$). Temperature of material surface reached maximum of $T_{max} \approx 1763°C$ which did not exceed melting point of WC ($T_{WC} \approx 2870°C$). It is important to mention that temperature in the melt pool could reach higher values. Despite that, temperature needed to melt carbide is over 1000°C higher than reported maximum value. However, due to excellent wettability of WC by liquid Ni, it is possible that fine ceramic reinforcement could be affected by partial dissolution. Due to pyrometer set – up, measurements were performed in fixed point on the sample. Because of that, obtained results shows how deposition of subsequent tracks and layers affect material temperature. It was observed, that exposition to temperatures higher than melting point of Inconel 625 are very short (about 1 – 1,5 second). Because of constant heating, microstructure of coating is affected and transformed due to prolonged time that enables grain growth.

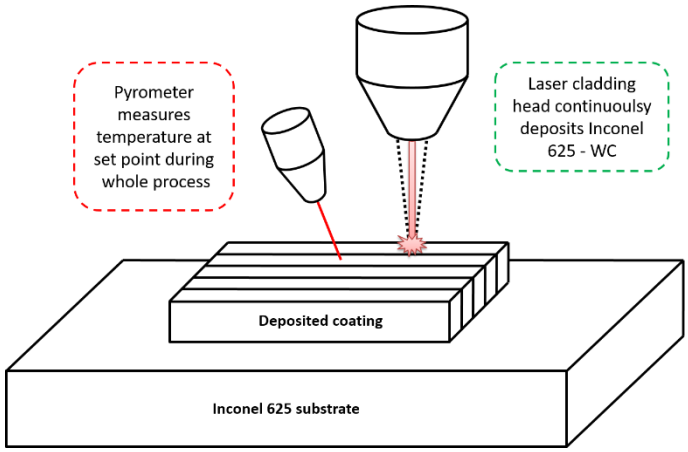

Fig. 10. *Radiation pyrometer set – up for temperature measurements*

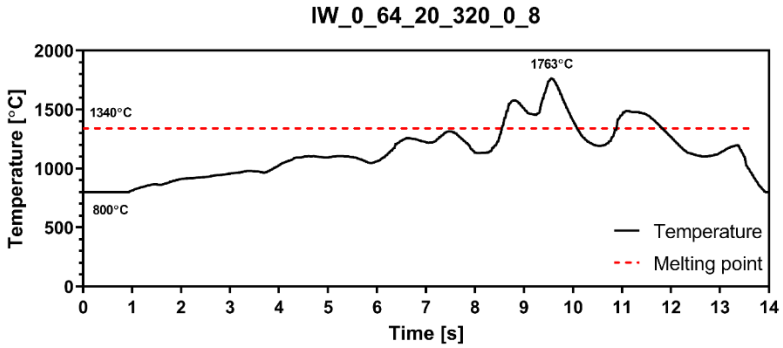

Fig. 11. *Temperature measurement of material surface obtained during laser cladding of Inconel 625 – WC_1 samples under 320 W laser power*

All of samples possess semicircular shape of sublayers. It is preserved in whole volume of material due to shape of melt pool produced as a result of laser action. Differences in microstructure are clearly visible between substrate and deposited Inconel 625 – WC composite. Coating is characterized by fine microstructure which was obtained

as a result of material supercooling. No delamination at coating – substrate boundary as presented below in Fig. 12.

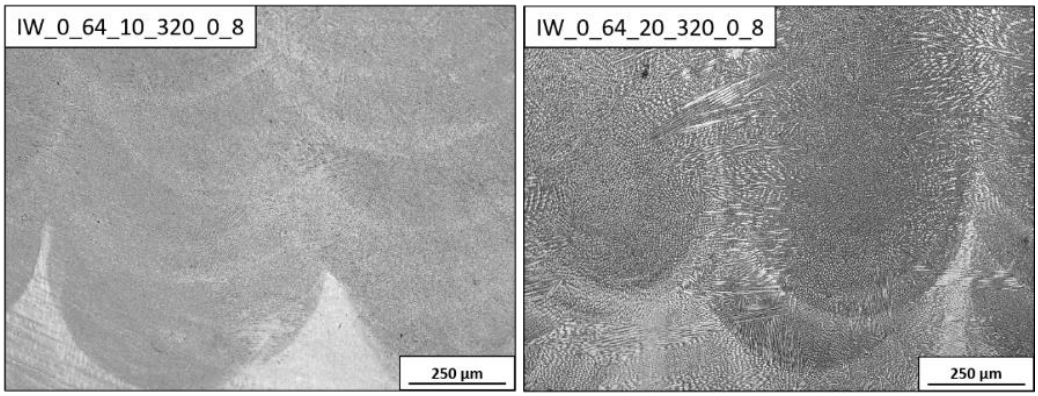

Fig. 12. *Inconel 625 – 10 and 20 wt % WC samples visible differences in microstructure between deposited tracks*

In order to investigate formation of secondary eutectic phase in IW_0_64_30_320_0_8 sample, SEM – EDS point analysis was conducted in order to check element concentration. As seen in Fig. 13 point analysis revealed comparable quantities of W in both investigated areas, which confirms partial dissolution of WC in Ni – based matrix. However, complete dissolution was prevented due to rapid nature of laser processing. The increased content of Nb, Mo and C in "white" phase indicates formation of secondary carbides with carbon that originated from dissolved WC and binder. As expected, "dark grey" matrix showed almost 60 wt % of Ni and depletion of previously mentioned Nb and Mo. It allows to conclude that element microsegregation occurred during solidification of deposited material. It has to be pointed out, that SEM EDS analysis affect areas around highlighted points, thus they must be treated accordingly. The wt % amounts shown in tables are approximates.

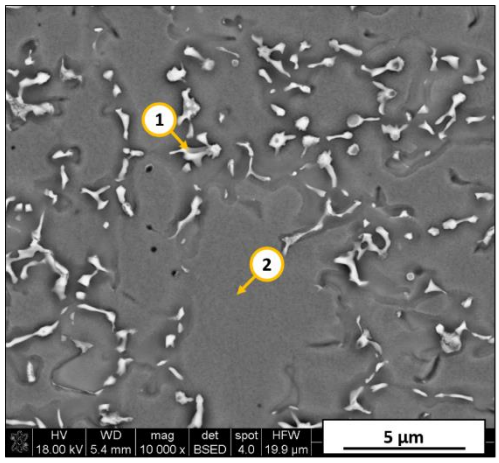

Element	Point 1 [wt %]	Point 2 [wt %]
C	7	3
O	1	1
Nb	9	2
Mo	17	7
Cr	17	17
Fe	1	2
Ni	37	58
W	11	10

Fig. 13. *Point SEM EDS analysis of IW_0_64_20_320_0_8 sample*

The second sample - IW_0_64_30_320_0_8 is shown in Fig. 14. As stated above, three distinct phases were present in the material. Clear differences in microstructure

allows to formulate a statement that introduction of 30 wt % of fine WC_1 powder into Inconel 625 alloy, resulted in major transformation of material. As seen in table with SEM EDS point analysis, precipitate highlighted as point 1 consisted of mostly W. Some amount of Ni was detected because of Ni matrix around precipitate. Fishbone – like structure highlighted as point 2, exhibited increased concentration of Cr, Mo and Nb with significant signal from W. This indicates formation of secondary phases during rapid solidification of coating. Composite matrix marked by point 3, showed similar results as for sample containing 20 wt % of WC. Higher content of Ni with depletion of Cr, Mo and Nb was detected in comparison to point 2. The fishbone – like structures observed in this sample are typical for eutectics which indicates that there could be more than one phase present in this type of structures. In order to confirm that samples were subjected to XRD analysis.

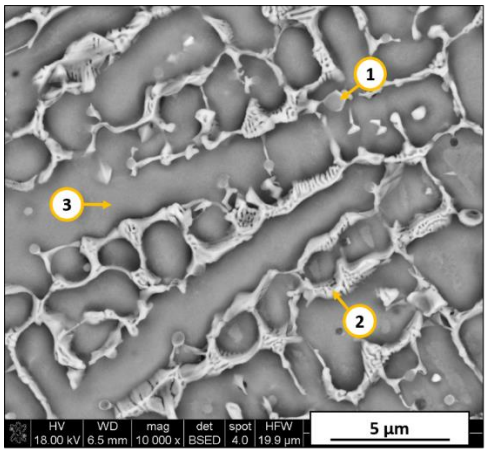

Element	Point 1 [wt %]	Point 2 [wt %]	Point 3 [wt %]
C	5	5	5
O	1	1	4
Nb	1	7	2
Mo	3	11	7
Cr	5	20	17
Fe	0	1	3
Ni	14	42	59
W	71	12	5

Fig. 14. *Point SEM EDS analysis of IW_0_64_30_320_0_8 sample*

The results obtained by XRD analysis are presented in Fig. 15. It shows that sample with addition of 20 wt % of WC consisted of austenitic γ – Ni and hexagonal WC which was added as reinforcement. The signal originating from WC was weak in comparison to γ – Ni. Next sample provided completely different results. Similarly to 20 wt % sample, both γ – Ni and hexagonal WC were detected. Additionally, appearance of other phases was observed. Formation of W_2C, $W_6C_{2,54}$ and $(W,Cr,Ni)_{23}C_6$ secondary carbides was possible due to partial dissolution of WC. Formation of NbC was indicated by detected weak signal. The presence of many secondary phases are possible because of formation of eutectic in material.

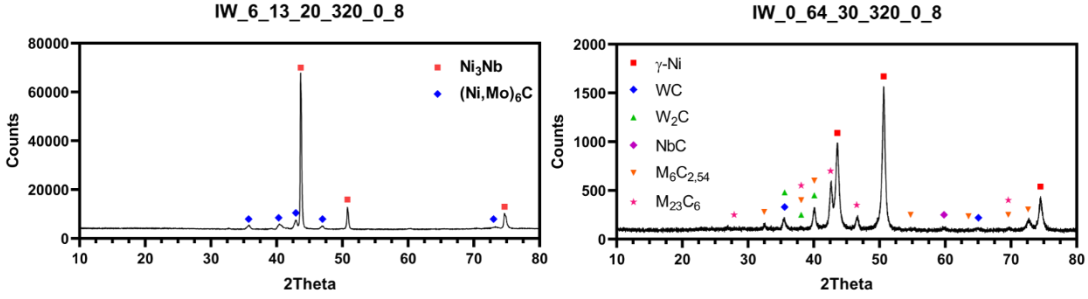

Fig. 15. *XRD phase analysis of IW_0_64_20_320_0_8 and IW_0_64_30_320_0_8 samples*

Obtained results from SEM - EDS mapping confirmed that element microsegregation of elements occurred. As seen in Fig. 16. Higher content of WC resulted in strong segregation effect in material. This sample exhibited significant presence of Mo, Nb and C, with small depletion of W at grain boundaries which indicates correlation between amount of introduced WC and formation of TCP phases. It can be observed that Mo and Nb shows strong chemical affinity with carbon. Dissolution of WC promoted formation of many secondary phases in this material, which is the result of high content of C introduced to system. Obtained results showed significant amount of W and Cr present in TCP phases.

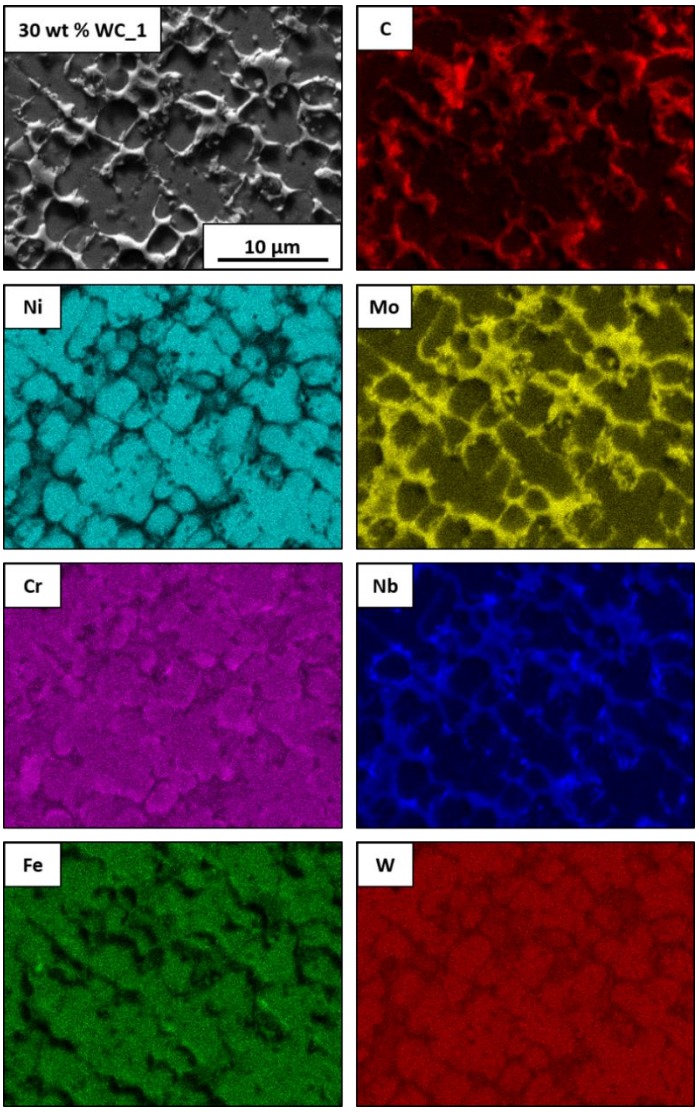

Fig. 16. *SEM EDS mapping of IW_0_64_30_320_0_8 sample, showing segregation of elements during laser cladding*

Based on analysis results, it was decided that further investigation of microstructure was necessary to further determine transformations of Inconel 625 – WC composite system during laser cladding. In order to obtain more information about phase

composition and microstructure, transmission electron microscopy (TEM) investigation was conducted on selected samples: IW_0_64_20_320_0_8 and IW_0_64_30_320_0_8.

Precipitates of TCP phases at grain boundaries were observed in Fig. 17. Area diffraction pattern in Fig. 17B, shows that all three visible matrix crystallites have similar crystallographic orientation which indicates oriented grain growth. The differences in orientation were most likely caused by formation of TCP phases precipitates between grains. It prevented parallel grain growth because of slight misorientation caused by their appearance between matrix grains. The observed net of black lines in the metal matrix reveals that large amount of dislocations were present in Inconel 625 – WC composite after deposition. They appear due to internal thermal stresses in material after rapid laser processing.

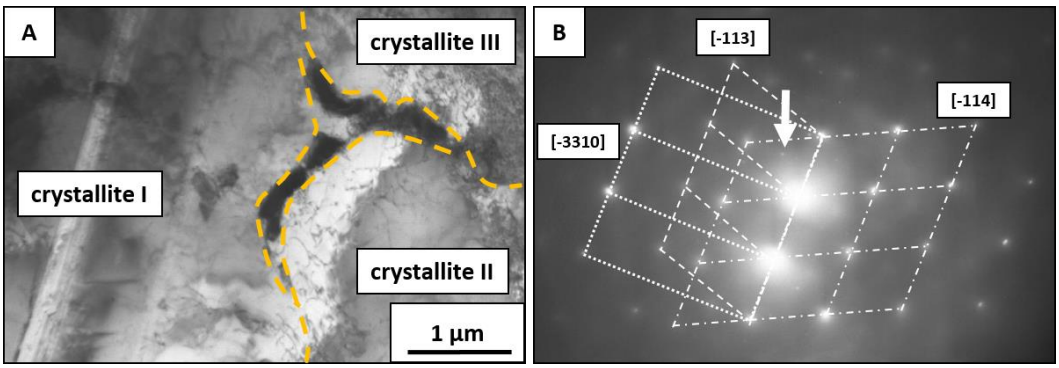

Fig. 17. *TEM bright field image of IW_0_64_20_320_0_8 sample with diffraction pattern of 3 Ni – based matrix crystallites*

In case of sample with 30 wt % addition of WC, material behavior was different. XRD and SEM results, already pointed microstructural and phase differences from sample with 20 wt % WC addition. TEM bright field image presented in Fig. 18, depicts even higher amount of dislocations in material. The TCP phases precipitates were larger and started to surround γ – Ni grains.

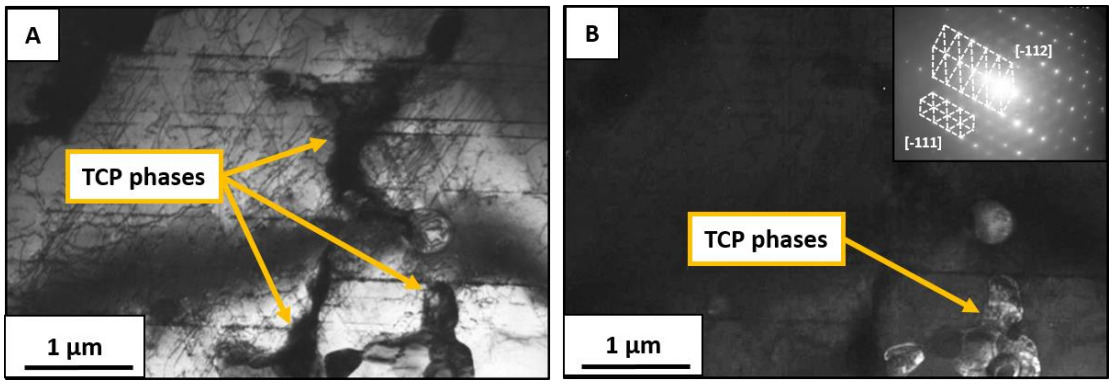

Fig. 18. *TEM bright and dark field images of IW_0_64_30_320_0_8 – TCP phases precipitates at grain boundary, visible net of dislocations*

Because of dissolution of fine WC particles (D_{WC_1} = 0,64 µm), it was decided to replace WC_1 powder with larger WC_4 powder (D_{WC_4} = 6,13 µm). This change was made in order to prevent dissolution of carbide in metal.

Hardness of each sample was measured throughout deposited coating. As presented in Fig. 19, sample with 30 wt % WC addition had significantly higher hardness than other materials. Smaller content of WC (10 and 20 wt %) did not increase hardness of the composite at all. It allowed to conclude that appearance of secondary phases like TCP was responsible for improvement of hardness as presented in Table 2. Nanohardness of specific phases was measured for sample with 30 wt % WC addition. The results showed that metal matrix had 306,2 ± 31,1 HV while phases at grain boundaries had 534,2 ± 34,4 HV. This indicates that microsegregation during solidification led to strong depletion of strengthening elements like Cr and Mo in γ - Ni matrix with simultaneous formation of hard but brittle phases at grain boundaries.

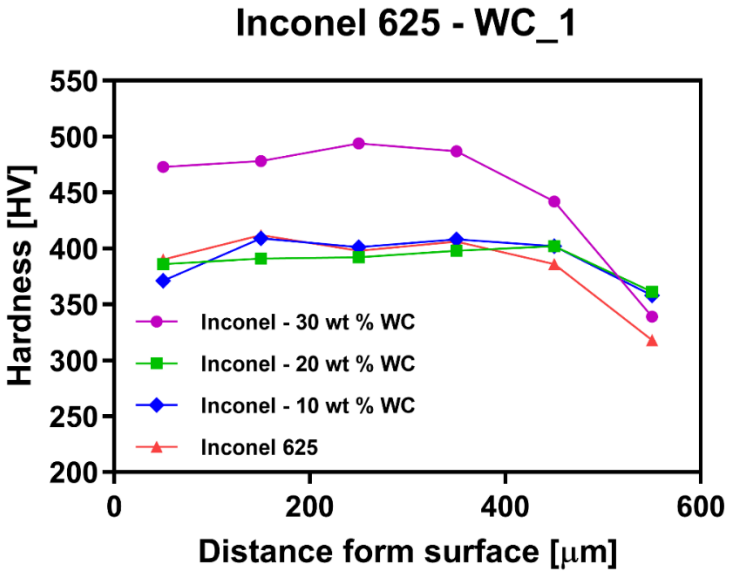

Fig. 19. *Hardness distribution thorough the coating in Inconel – WC_1 samples*

Table 2. *Measured hardness of Inconel – WC_1 samples with nanohardness of two distinct phases in Inconel 625- WC_1 30 wt % sample*

Material	**Average hardness [HV]**
Inconel 625	396,3 ± 10,5
Inconel 625 – WC_1 10 wt %	396,2 ± 15,3
Inconel 625 – WC_1 20 wt %	397,2 ± 6,1
Inconel 625 – WC_1 30 wt %	469,9 ± 24,9
Area in 625 – WC_1 30 wt %	**Nanohardness [HV]**
Grain boundaries	534,2 ± 34,4
γ – Ni matrix	306,2 ± 31,1

7. Laser cladding of Inconel 625 – WC (D_{WC_4} = 6,13 µm)

Tungsten carbide powder with D_{WC_4} = 6,13 µm, was selected for second batch powder mixtures. Preparation methodology was exactly the same the same as for WC_1 powder which was described above. Powder mixtures with different WC powder content were made as shown in Table 3. No powder with 30 wt % of WC was prepared in order to avoid excessive formation of TCP phases in material during laser cladding. The result of powder homogenization is shown in Fig. 20.

***Table 3**. Compositions of powder mixtures made with WC_4 powder*

Powder mixture	Inconel 625 [wt %]	WC [wt %]	Carbon content [wt %]
Inc_WC10_6_13	90	10	0,61
Inc_WC20_6_13	80	20	1,22

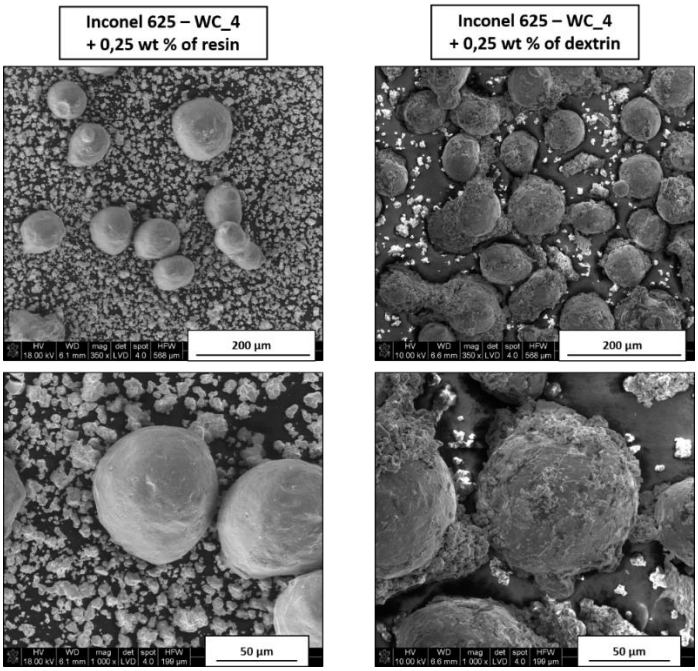

***Fig. 20.** Powder mixtures with 0,25% wt % resin (left) and 0,25 wt % dextrin (right) after 90 min of homogenization*

Obtained powder mixtures with dextrin binder were used for laser cladding. Processing parameters were analogical to samples with addition of WC_1 powder after optimization and are shown in Table 4.

***Table 4.** Laser cladding parameters for samples with addition of WC_4 powder*

Sample ID	WC content [wt %]	Laser power [W]	Distance between tracks - S_{BT} [mm]
IW_6_13_10_320_0_8	10	320	0,8
IW_6_13_10_320_0_8	20	320	0,8

SEM investigations of parallel and perpendicular to tracks cross – sections are presented in Fig. 21. Both samples looked similar with no significant differences in microstructure. Because of that, sample IW_6_13_320_0_8 was selected to be shown in order to represent material behavior during laser cladding. Three distinct areas were visible: deposited coating, Inconel 625 substrate and transitional (interlayer) area, which formed in result of mixing of both materials in the melt pool during laser processing. Microstructure of coating was refined in comparison to substrate material. It was observed that precipitates formation occurred at grain boundaries of γ - Ni matrix grains in both transitional area and deposited coating. As presented in Fig. 21C shows boundary between sublayers. It was observed that some of introduced WC grains survived laser cladding due to their larger size. In Fig. 21D agglomeration of angular WC was reported in close proximity to fishbone – like structure of TCP phases precipitates despite lower content of WC in material.

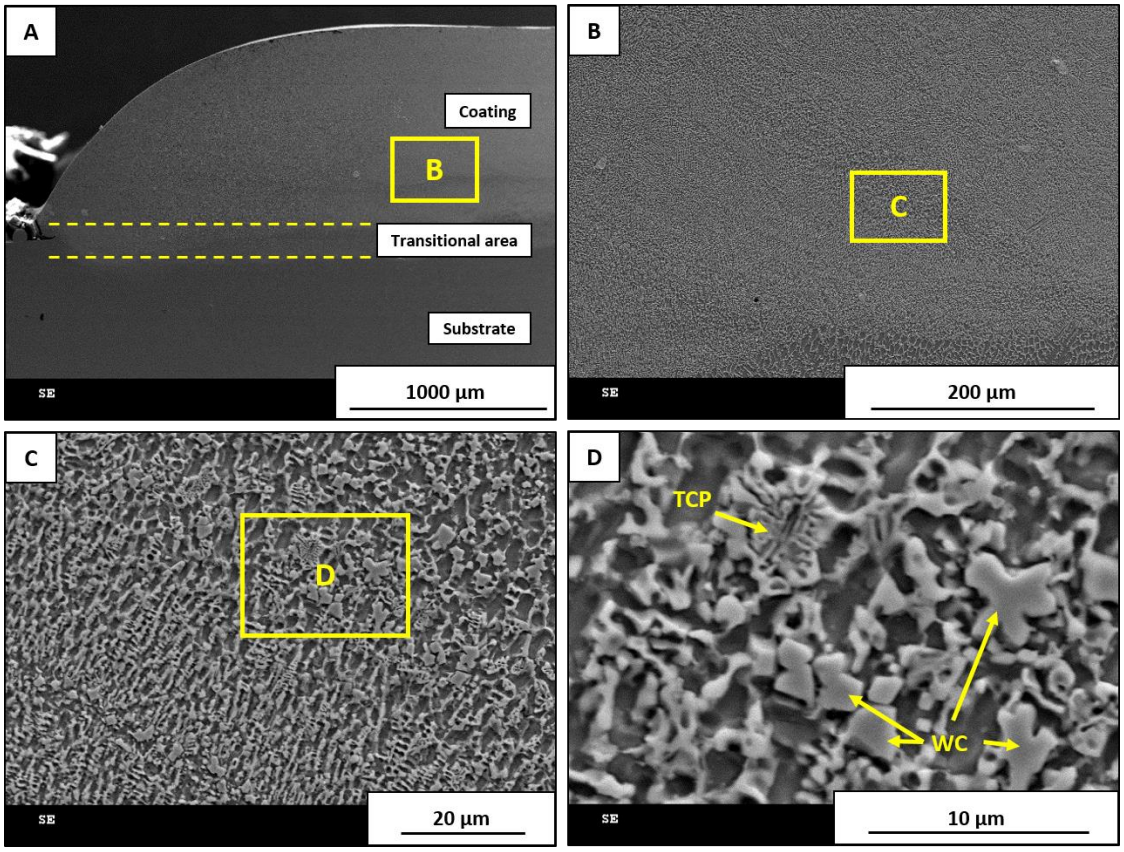

Fig. 21. *Parallel to tracks cross – section of IW_6_13_20_320_0_8*

As presented in Fig. 22, obtained coating material possess complex microstructure. According to Fig. 22C it was evident that WC grains survived laser cladding. The dissolution of carbide particles started at the tips of angular WC grains which promoted formation of fishbone – like eutectic structures of TCP phases. As it is seen in Fig. 22D, microstructure transformation did not allow result in clear boundaries between elongated grains and other secondary phases structures.

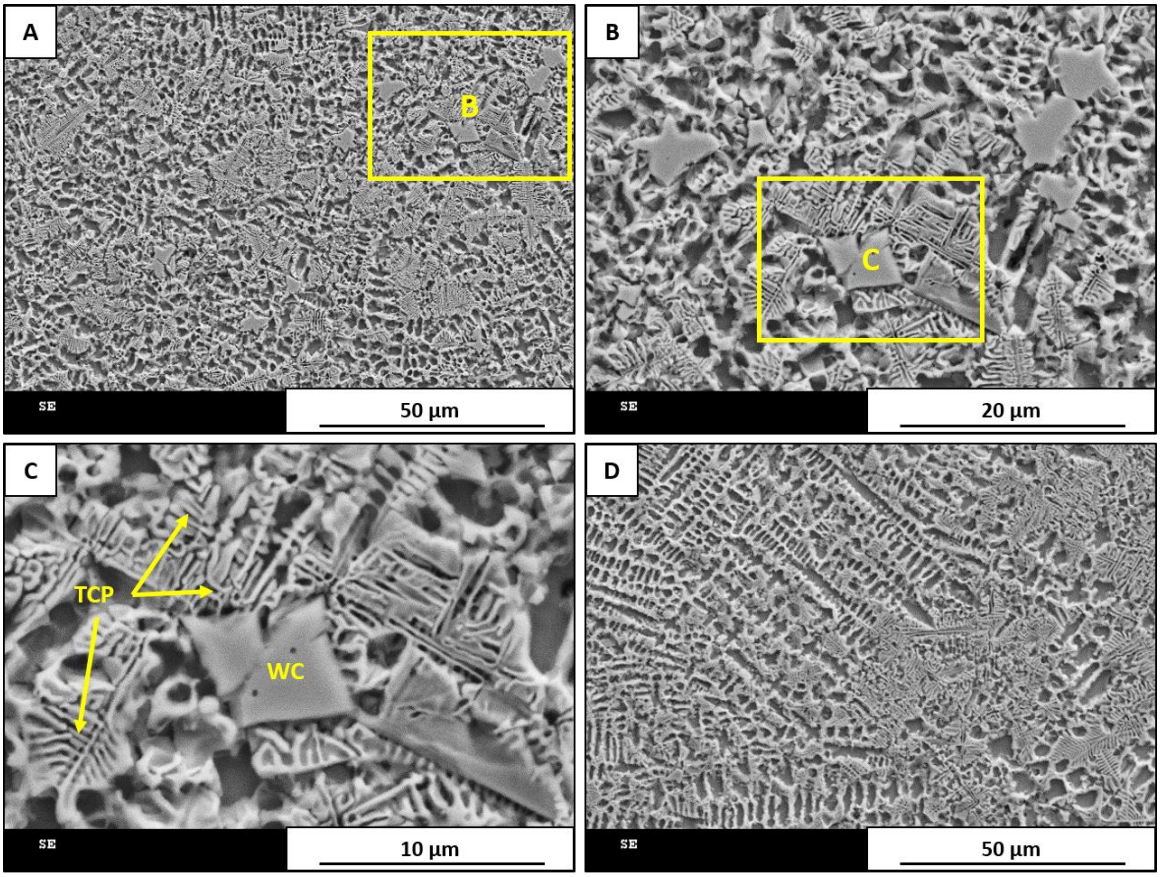

Fig. 22. *Parallel to tracks cross – section of IW_6_13_20_320_0_8 – visible WC grains with TCP phases fishbone – like structures*

Temperature measurements for IW_6_13_320_0_2 sample in set point, revealed that process provides sufficient energy for melting of Inconel 625 as presented in Fig. 23. Repetitive laser action in area close to measured point confirmed exposure to temperatures over 1000°C for about 10 seconds which promoted longitudinal grain growth because of temperature gradients differences in material.

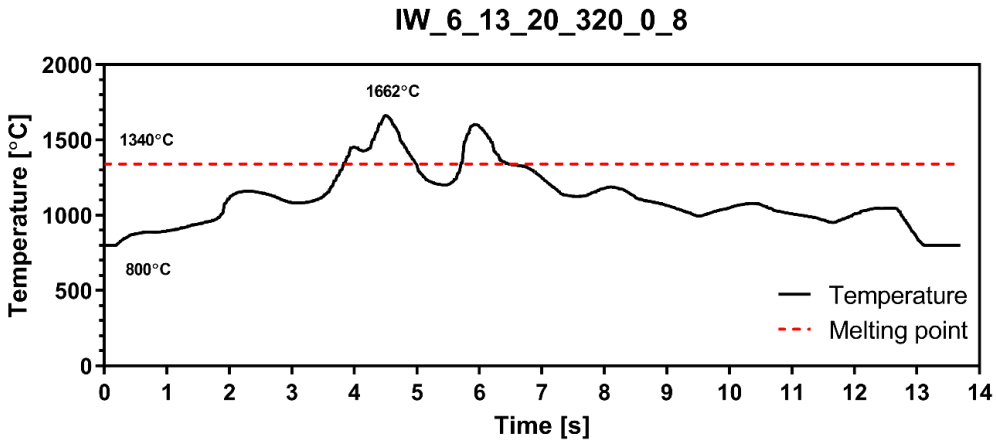

Fig. 23. *Representative temperature measurement on material surface for laser cladding of Inconel 625 – WC_4 samples*

TEM investigations of different areas of sample provided valuable information about material. The TEM – EDS point analysis is shown in Fig. 24. together with table presenting element concentration in specific areas. Seven distinct regions were subjected to element point analysis. It is important to remember that results obtained by this method can be distorted by contaminations, originated from other phases. As the electron beam passes through the material other phases can interfere and provide signals detected by TEM. Obtained results were summarized in the Table 5. Point 1 showed high wt and at. % content of Ni together with typical for Inconel 625 alloy content of Cr and Mo. This confirmed that light-gray area represented γ – Ni matrix of deposited coating. Analysis of points 2, 3 and 4 revealed high amount of W at over 59 at. % of each. This indicated that these areas were residual undissolved WC grains introduced as reinforcement to the material. Cr amount was increased in areas 5, 6 and 7 at 22 – 24 at. % as a result f of secondary phases formation. This was also true for Mo, which behaved similarly to Cr. Weak signal derived from Nb was detected in all analyzed areas at level of 1 – 3 at. %, except for point 1.

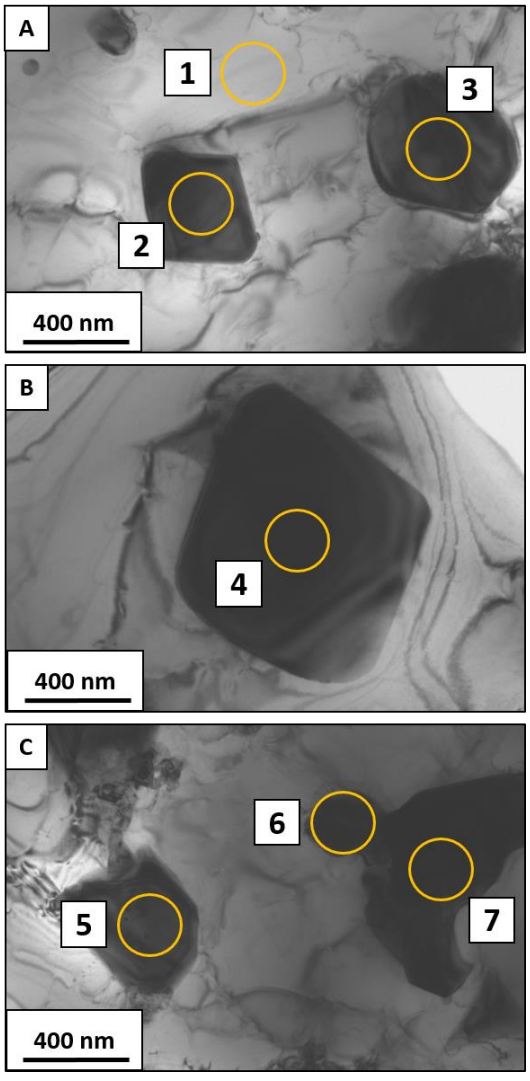

Fig. 24. *TEM bright field images of IW_6_13_20_320_0_8 sample with EDS point analysis results*

Table 5. *TEM EDS point analysis of areas shown in Fig. 24*

Point ID		Ni	Cr	Mo	Nb	W	Fe
Point 1	**[wt %]**	73	13	3	0	10	0
	[at %]	78	16	2	0	4	0
Point 2	**[wt %]**	35	11	8	2	44	0
	[at %]	13	5	2	1	79	0
Point 3	**[wt %]**	29	10	8	2	50	1
	[at %]	19	7	3	1	69	1
Point 4	**[wt %]**	30	6	7	3	54	0
	[at %]	24	8	6	3	59	0
Point 5	**wt %]**	46	17	13	4	20	0
	[at %]	56	24	10	3	7	0
Point 6	**[wt %]**	50	16	10	2	21	1
	[at %]	60	22	8	1	8	1
Point 7	**[wt %]**	45	17	13	2	23	0
	[at %]	56	24	10	1	9	0

As shown in Fig. 25, the addition of WC and formation of secondary phases were beneficial for overall hardness of deposited material. The average hardness of the Inconel 625 – 10 and 20 wt % WC coatings was about 31 – 32% higher than that of pure Inconel 625 obtained by the same technique (Table 6). Decline in hardness was observed in areas closer to coating/substrate boundary because of mutual mixing between substrate and powders in melt pool.

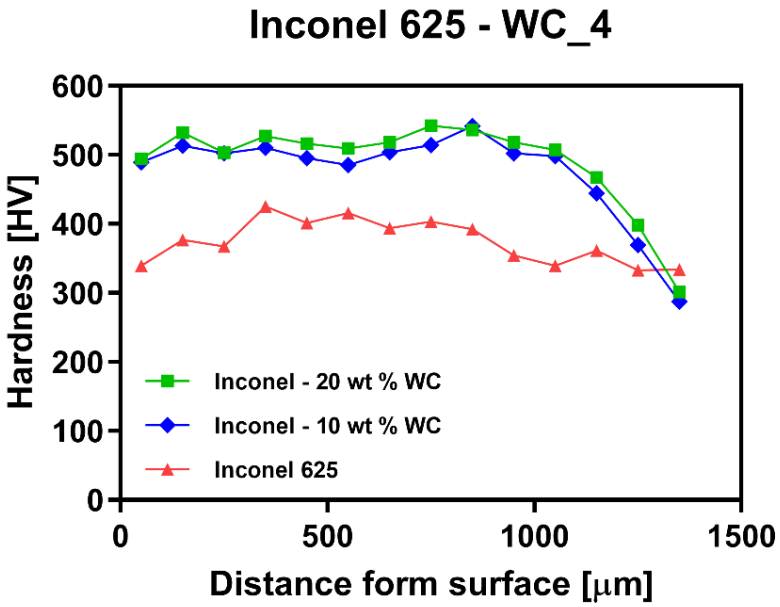

Fig. 25. *Hardness distribution thorough the coating in Inconel – WC_4 samples*

Table 6. *Measured hardness of Inconel – WC_4 samples*

Material	Hardness [HV]
Inconel 625 – WC_4 20 wt %	502,6 ± 34,1
Inconel 625 – WC_4 10 wt %	499,9 ± 22,9
Inconel 625	380,8 ± 28,9

8. Heating rate effect on microstructure of Inconel 625 – WC system

The analysis of Inconel 625 – WC composite obtained by laser cladding proved that it is a promising method of production of this type of materials. However, due to complexity of the system, analysis of microstructure and phase composition of the material was challenging. For better understanding how material behaves while exposed to different heating conditions, powder mixtures were subjected to Differential Thermal Analysis (DTA). This allowed to investigate how different heating rate affected microstructure transformation. Table DTA presents list of samples and conditions of analysis. Mixtures with addition of WC_2 (D_{WC_2} = 3,88 μm) and WC_4 (D_{WC_4} = 6,13 μm) powder mixtures were prepared by the same procedure as described in Chapter 9.1. Small amount of each powder were put inside distinct Al_2O_3 crucible and then were individually analyzed in temperature up to 1450°C. List of prepared samples is presented in Table 7.

Table 7. *List of samples subjected to DTA analysis with analysis conditions*

Sample	WC powder	WC diameter [μm]	WC content [wt %]	Heating rate [°C/min]
Inc_10	-	-	-	10
Inc_30	-	-	-	30
WC_2_10_10	WC_2	3,88	10	10
WC_2_10_30	WC_2	3,88	10	30
WC_2_20_10	WC_2	3,88	20	10
WC_2_20_30	WC_2	3,88	20	30
WC_2_30_10	WC_2	3,88	30	10
WC_2_30_30	WC_2	3,88	30	30
WC_4_10_10	WC_4	6,13	10	10
WC_4_10_30	WC_4	6,13	10	30
WC_4_20_10	WC_4	6,13	20	10
WC_4_20_30	WC_4	6,13	20	30
WC_4_30_10	WC_4	6,13	30	10
WC_4_30_30	WC_4	6,13	30	30

All of obtained samples were grinded and polished in order to provide surface with good quality suitable for SEM – EDS examination. SEM - EDS point analysis was conducted in marked areas in order to check their average element composition. SEM images are shown in Fig. 26 and 27. All of examined samples had some amount of porosity in form of small circular black areas. They appeared due to evaporation of dextrin binder or as a result of gas confinement during melting process. All samples were coated by thin carbon layer in order to improve its conductivity which is necessary for SEM analysis. It must be pointed out that it made analysis of carbon content not accurate. However, the measured amount of carbon in specific area, still can generally indicate its high or low content.

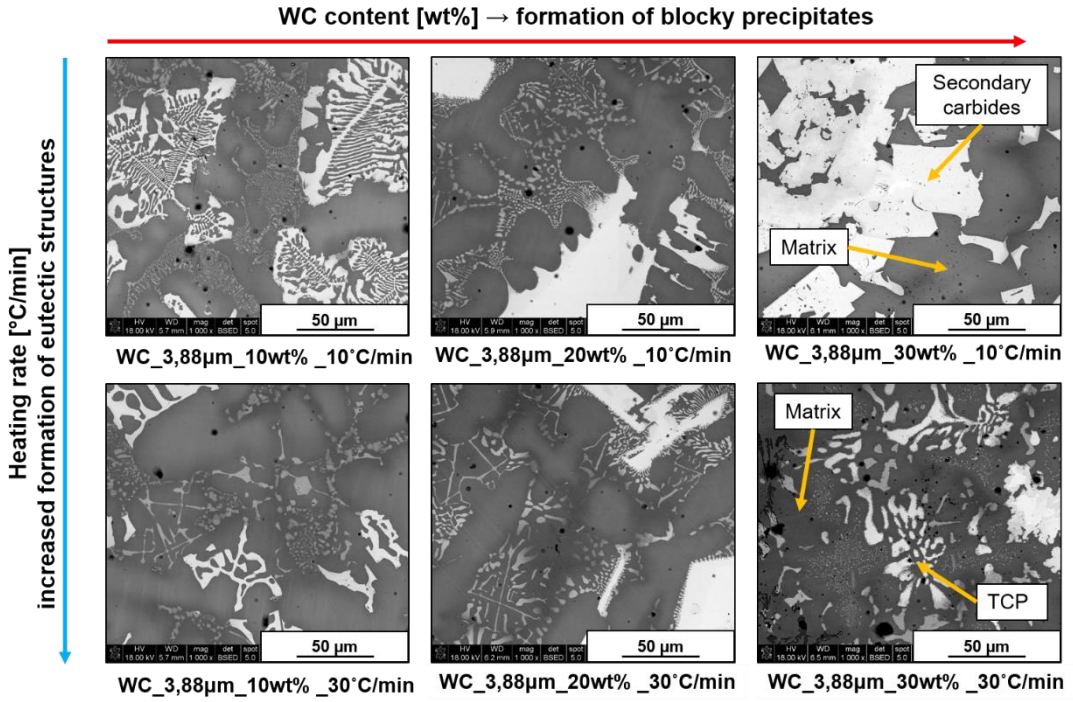

Fig. 26. *SEM images of DTA melted Inconel 625 – WC 3,88 µm powder mixtures*

As it is shown in Fig. 26, both heating rate and WC weight content have significant influence on microstructure of obtained material. Low heating rate of 10°C/min allowed formation of eutectic structures in 10 and 20 wt % of WC samples. On the contrary sample containing 30 wt % of WC showed presence of fully developed precipitates blocky secondary carbides. In case of faster heating rate of 30°C/min, obtained materials had less time to complete formation of precipitates. Observed materials are characterized by structures which development was stopped by fast heating followed by rapid cooling of material. In case of 30 wt % material heated in 30°C/min – no formation of blocky precipitates was visible in favor of irregular TCP phases structures.

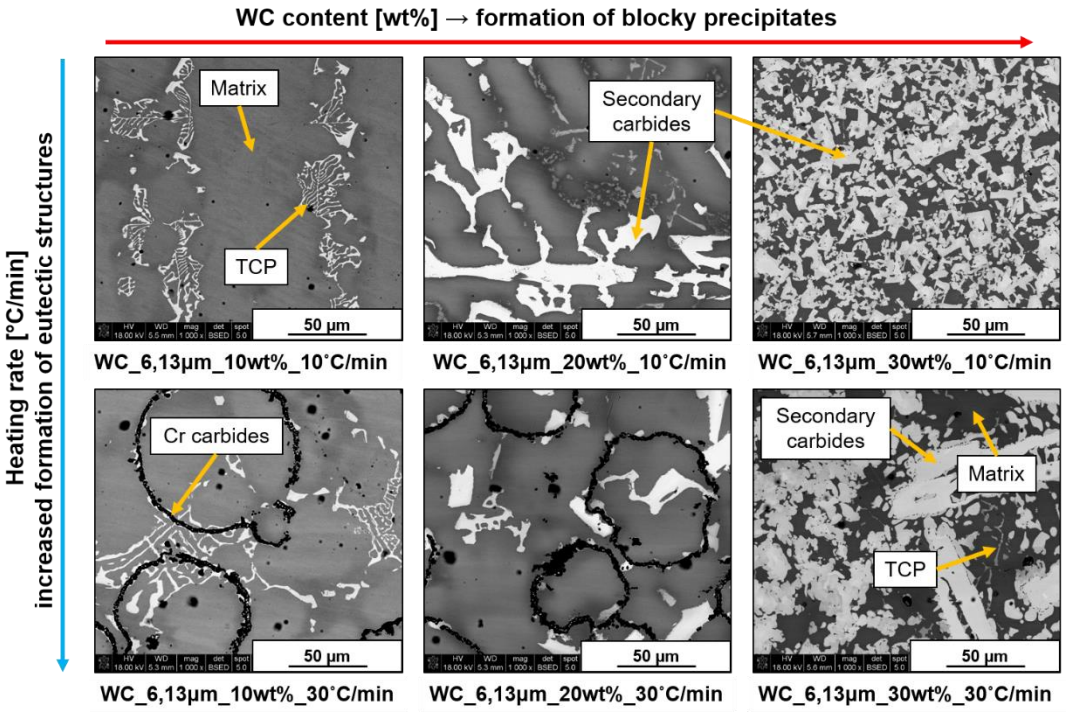

Fig. 27. *SEM images of DTA melted Inconel 625 – WC 6,13 µm powder mixtures*

Samples made by controlled melting of powder mixtures containing larger WC particles, showed similar behavior to previously shown materials – Fig. 27. The obtained microstructure was finer especially for sample 30 wt % of WC heated by 10°C/min. For 10 and 20 wt % of WC by 30°C/min, formation of characteristic "black circles" was observed around unmelted Inconel 625 particles. It occurred due to segregation of Cr from alloy to surface of Inconel grains which was followed by reaction with carbon. It prevented melting of metal grains during thermal processing.

Hardness analysis were performed on all DTA prepared samples - Fig. 28. Because of fine structures of secondary eutectic structures in some materials, it was not possible to measure their hardness. The graphs shows maximum of three distinct phases where: *"matrix"* – stands for Ni – based matrix of the material, *"irregular"* – stands for fine irregular precipitates of secondary phases while *"blocky"* – stands for large blocky precipitates in some samples. Average values for each sample is presented in Table 8.

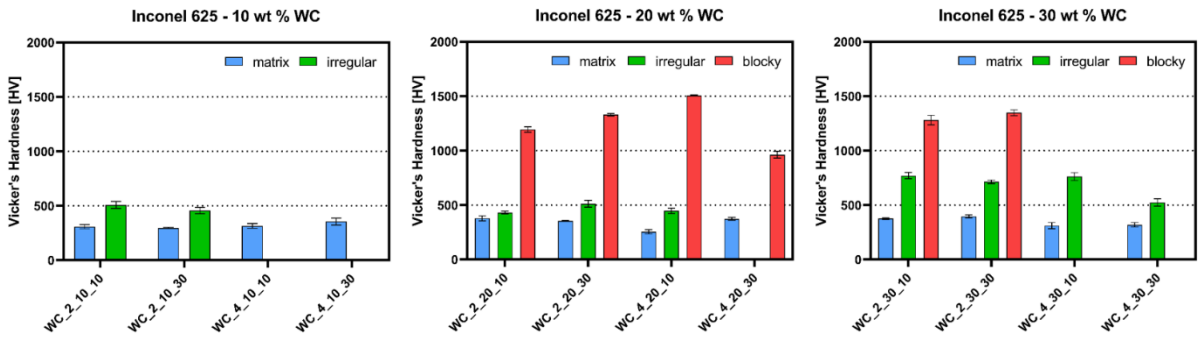

Fig. 28. *Hardness of disctinct phases in samples made with controlled heating rate (DTA)*

Table 8. *Average hardness of phases in DTA obtained Inconel 625 -WC samples*

Sample ID	Average hardness [HV]		
	matrix	irregular	blocky
WC_2_10_10	308,64 ± 18,45	508,19 ± 31,77	-
WC_2_10_30	296,21 ±6,47	456,23 ± 28,16	-
WC_4_10_10	316,83 ±22,51	-	-
WC_4_10_30	356,01 ±31,03	-	-
WC_2_20_10	379,12 ±23,13	430,84 ± 13,43	1194,45 ± 24,28
WC_2_20_30	355,76 ± 3,54	512,67 ± 31,82	1330,20 ± 12,02
WC_4_20_10	255,52 ± 19,09	448,61 ± 24,74	1507,48 ± 4,37
WC_4_20_30	374,76 ± 12,51	-	962,28 ± 31,32
WC_2_30_10	376,13 ± 6,87	770,65 ± 29,15	1281,71 ± 43,94
WC_2_30_30	397,15 ±13,95	714,81 ± 16,42	1348,74 ± 26,11
WC_4_30_10	312,98 ± 27,62	762,29 ± 35,47	-
WC_4_30_30	319,73 ± 20,38	524,40 ± 34,69	-

Collected results clearly shows that secondary phases had higher hardness than Ni – based matrix. Different WC particle size and heating rate affected formation of precipitates which in consequence changed hardness of distinct phases in obtained materials. Significant increase in hardness values for irregular eutectic precipitates was observed between 20 and 30 wt % WC addition samples. This indicates that higher amount of WC promotes precipitation strengthening of Inconel 625 – WC system.

Conclusions

To conclude, laser cladding can be successfully implemented as an additive manufacturing method for Inconel 625 – WC composite system. Careful optimization of processing parameters are necessary in order to ensure and guarantee high quality of obtained material. However, experiments confirmed that it needs to be performed or adjusted in case of different powder compositions and/or laser apparatus. Laser cladding of Inconel 625 – WC system confirmed that:

- Good quality of material can be achieved by individual optimization of laser cladding process parameters
- WC addition allowed extensive formation of secondary TCP phases that usually appear after extensive heat treatment
- It is possible to prevent complete WC dissolution in Ni – based liquid alloy by manipulation of particle size and process parameters
- Average hardness of composite was increased due to addition of WC particles. It was possible because of microsegregation of alloying elements like Mo and Nb and their reactions with C originated from partially dissolved WC

- Precipitation strengthening of composite was observed by formation of various secondary phases including intermetallic TCP phases and carbides of alloying elements
- Higher heating rates prevents complete dissolution of larger WC grains and stops full development of TCP phases precipitates, which leaves them in thermodynamically non - equilibrium state
- Precipitates of TCP phases and secondary carbides are much harder and more brittle than γ – Ni matrix
- It is needed to carefully optimize and/or adjust process parameters for different laser sources. The quality of obtained coating cannot be guaranteed by using parameters optimized for different laser apparatus.
- It is possible to obtain good quality of material using low laser power of about ≈ 300 W

Obtained results concludes that **Inconel 625 – WC composite system is suitable for laser additive manufacturing**.

Bibliography

[1] T. Teppernegg, T. Klünsner, C. Kremsner, C. Tritremmel, C. Czettl, S. Puchegger, S. Marsoner, R. Pippan, R. Ebner, High temperature mechanical properties of WC-Co hard metals, Int. J. Refract. Met. Hard Mater. 56 (2016) 139–144. doi:10.1016/j.ijrmhm.2016.01.002.

[2] G.P. Dinda, A.K. Dasgupta, J. Mazumder, Laser aided direct metal deposition of Inconel 625 superalloy: Microstructural evolution and thermal stability, Mater. Sci. Eng. A. 509 (2009) 98–104. doi:10.1016/j.msea.2009.01.009.

[3] S. Zhou, X. Dai, X. Zeng, Effects of processing parameters on structure of Ni-based WC composite coatings during laser induction hybrid rapid cladding, Appl. Surf. Sci. 255 (2009) 8494–8500. doi:10.1016/j.apsusc.2009.05.161.

[4] J.R. (Joseph R.. Davis, ASM International. Handbook Committee., Heat-resistant materials, ASM International, 1997. https://www.asminternational.org/search/-/journal_content/56/10192/16857762/PUBLICATION (accessed October 15, 2019).

[5] S. Tosto, F. Pierdominici, M. Bianco, Laser cladding and alloying of a Ni-base superalloy on plain carbon steel, J. Mater. Sci. 29 (1994) 504–509. doi:10.1007/BF01162514.

[6] M. Riddihough, Stellite as a wear-resistant material, Tribology. 3 (1970) 211–215. doi:10.1016/0041-2678(70)90058-8.

[7] X. Zhang, X. Jie, L. Zhang, S. Luo, Q. Zheng, Improving the high-temperature oxidation resistance of H13 steel by laser cladding with a WC/Co-Cr alloy coating, Anti-Corrosion Methods Mater. 63 (2016) 171–176. doi:10.1108/ACMM-11-2015-1606.

[8] D.L. Olson, T.A. Siewert, S. Liu, G.R. Edwards, eds., Welding, Brazing and Soldering, ASM International, 1993. doi:10.31399/asm.hb.v06.9781627081733.

[9] K.P. Cooper, P. Slebodnick, Recent Developments in Laser Melt/Particle Injection Processing, J. Laser Appl. 1 (1989) 21–29. doi:10.2351/1.4745241.

[10] J. Przybylowicz, J. Kusinski, Laser cladding and erosive wear of Co-Mo-Cr-Si coatings, Surf. Coatings Technol. 125 (2000) 13–18. doi:10.1016/S0257-8972(99)00563-0.

[11] P.L. Hurricks, Some aspects of the metallurgy and wear resistance of surface coatings, Wear. 22 (1972) 291–320. doi:10.1016/0043-1648(72)90391-2.

[12] J. Przybyłowicz, J. Kusiński, Structure of laser cladded tungsten carbide composite coatings, J. Mater. Process. Technol. 109 (2001) 154–160. doi:10.1016/S0924-0136(00)00790-1.

[13] J. Kusiński, Lasery i ich zastosowanie w inżynierii materiałowej, Wydaw. Naukowe “Akapit,” 2000.

https://polona.pl/item/lasery-i-ich-zastosowanie-w-inzynierii-materialowej,Mzk5NDM3Mw/#info:metadata (accessed October 15, 2019).

[14] J. DuPont N., J. Lippold C., S. Kiser D., Welding Metallurgy and Weldabilidy of Nickel Based Alloys, Wiley, 2009.

[15] A.I. Dashchenko, ed., Manufacturing Technologies for Machines of the Future, Springer Berlin Heidelberg, Berlin, Heidelberg, 2003. doi:10.1007/978-3-642-55776-7.

[16] D.-G. Ahn, Direct metal additive manufacturing processes and their sustainable applications for green technology: A review, Int. J. Precis. Eng. Manuf. Technol. 3 (2016) 381–395. doi:10.1007/s40684-016-0048-9.

[17] S. Khademzadeh, N. Parvin, P.F. Bariani, Production of NiTi alloy by direct metal deposition of mechanically alloyed powder mixtures, Int. J. Precis. Eng. Manuf. 16 (2015) 2333–2338. doi:10.1007/s12541-015-0300-1.

[18] D.M. Hensinger, A.L. Ames, J.L. Kuhlmann, Motion planning for a direct metal deposition rapid prototyping system, in: Proc. 2000 ICRA. Millenn. Conf. IEEE Int. Conf. Robot. Autom. Symp. Proc. (Cat. No.00CH37065), IEEE, n.d.: pp. 3095–3100. doi:10.1109/ROBOT.2000.845139.

[19] R. Dwivedi, R. Kovacevic, Process planning for multi-directional laser-based direct metal deposition, Proc. Inst. Mech. Eng. Part C J. Mech. Eng. Sci. 222 (2008) 2517–2519. doi:10.1177/095440620822201203.

[20] F. Lia, J. Park, J. Tressler, R. Martukanitz, Partitioning of laser energy during directed energy deposition, Addit. Manuf. 18 (2017) 31–39. doi:10.1016/j.addma.2017.08.012.

[21] A. Dass, A. Moridi, State of the Art in Directed Energy Deposition: From Additive Manufacturing to Materials Design, Coatings. 9 (2019) 418. doi:10.3390/coatings9070418.

[22] M. CIESLAK, The welding and solidification metallurgy of alloy 625, Weld. J. 70 (1991) 49.

[23] M.J. Cieslak, G.A. Knorovsky, T.J. Headley, A.D. Romig, The use of new PHACOMP in understanding the solidification microstructure of nickel base alloy weld metal, Metall. Trans. A. 17 (1986) 2107–2116. doi:10.1007/BF02645909.

[24] M.J. Cieslak, T.J. Headley, T. Kollie, A.D. Romig, Melting and solidification study of Alloy 625, Metall. Trans. A, Phys. Metall. Mater. Sci. 19 A (1988) 2319–2331. doi:10.1007/BF02645056.

[25] J.N. DuPont, C.V. Robino, A.R. Marder, M.R. Notis, J.R. Michael, Solidification of Nb - Bearing Superalloys: Part I. Reaction Sequences, Metall. Mater. Trans. A. 29A (1988) 2785–2796.

[26] J.N. DuPont, C.V. Robino, A.R. Marder, Solidification of Nb - Bearing Superalloys: Part II. Pseudo Ternary Solidification Surfaces, Metall. Mater. Trans. A. 29A (1998) 2797–2806.

[27] C.E. Stevens, R.W. Ross, Production, fabrication, and performance of alloy 625 clad steel for aggressive corrosive environments, J. Mater. Energy Syst. 8 (1986) 7–16. doi:10.1007/BF02833455.

[28] R.J.L. Andon, J.F. Martin, K.C. Mills, T.R. Jenkins, Heat capacity and entropy of tungsten carbide, J. Chem. Thermodyn. 7 (1975) 1079–1084. doi:10.1016/0021-9614(75)90241-4.

[29] L. Brewer, R.H. Lamoreaux, Thermochemical Properties., in: Molybdenum Physico-Chemical Prop. Its Compd. Alloy., 1980: pp. 7–191.

[30] Y.A. Chang, Thermal Properties of Tantalum Monocarbide and Tungsten Monocarbide, Trans. Metall. Soc. AIME. 239 (1967) 1685–1691.

[31] M.W. Chase, J.L. Curnutt, R.A. McDonald, H. Prophet, A.. Syverud, JANAF Thermochemical Tables, 7 (1975) 1–175.

[32] D.K. Gupta, L.L. Seigle, Free energies of formation of WC and W2C, and the thermodynamic properties of carbon in solid tungsten, Metall. Trans. A. 6 (1975) 1939–1944. doi:10.1007/BF02646859.

[33] K.K. Kelley, F.S. Boericke, G.E. Moore, E.. Huffman, W.M. Bangert, Thermodynamic Properties of Carbides of Chromium, USBM TP. 662 (1944) 43.

[34] L.S. Levinson, High-temperature heat content of tungsten carbide and hafnium carbide, J. Chem. Phys. 40 (1964) 1437–1438. doi:10.1063/1.1725330.

[35] A.D. Mah, Heats of combustion and formation of carbides of tungsten and molybdenum, 1963. http://www.osti.gov/energycitations/product.biblio.jsp?osti_id=7213401.

[36] A.D. Mah, Heats of Formation of Chromium Carbides, 1969.

[37] R.A. Oriani, W.K. Murphy, The Heat Capacity of Chromium Carbide (Cr3C2), J. Am. Chem. Soc. 76 (1954) 343–345. doi:10.1021/ja01631a007.

[38] H.. Schick, Thermodynamics of Ceratain Refractory Compounds, 1966.

[39] D.. Wagman, W.H. Evans, V.B. Parker, I. Halow, S.M. Bailey, R.H. Schumm, K.L. Churney, Selected Values of Chemical Thermodynamic Properties. Tables for Elements 54 Through 61 in the Standard Order of Arrangement, NBS Technol. Note. 270 (1971) 49.

[40] S. Zhou, J. Lei, X. Dai, J. Guo, Z. Gu, H. Pan, A comparative study of the structure and wear resistance of NiCrBSi/50 wt.% WC composite coatings by laser cladding and laser induction hybrid cladding, Int. J. Refract. Met. Hard Mater. 60 (2016) 17–27. doi:10.1016/j.ijrmhm.2016.06.019.

[41] S.W. Huang, M. Samandi, M. Brandt, Abrasive wear performance and microstructure of laser clad WC/Ni layers, Wear. 256 (2004) 1095–1105. doi:10.1016/S0043-1648(03)00526-X.

[42] S. Ghorbanpour, M.E. Alam, N.C. Ferreri, A. Kumar, B.A. McWilliams, S.C. Vogel, J. Bicknell, I.J. Beyerlein, M. Knezevic, Experimental characterization and crystal plasticity modeling of anisotropy, tension-compression asymmetry, and texture evolution of additively manufactured Inconel 718 at room and elevated temperatures, Int. J. Plast. (2019). doi:10.1016/j.ijplas.2019.09.002.

[43] Y.L. Hu, X. Lin, S.Y. Zhang, Y.M. Jiang, X.F. Lu, H.O. Yang, W.D. Huang, Effect of solution heat treatment on the microstructure and mechanical properties of Inconel 625 superalloy fabricated by laser solid forming, J. Alloys Compd. 767 (2018) 330–344. doi:10.1016/j.jallcom.2018.07.087.

[44] F. Silva, J. Santos, R. Gouveia, Dissolution of Grain Boundary Carbides by the Effect of Solution Annealing Heat Treatment and Aging Treatment on Heat-Resistant Cast Steel HK30, Metals (Basel). 7 (2017) 251. doi:10.3390/met7070251.

[45] M. Naghiyan Fesharaki, R. Shoja-Razavi, H.A. Mansouri, H. Jamali, Microstructure investigation of Inconel 625 coating obtained by laser cladding and TIG cladding methods, Surf. Coatings Technol. 353 (2018) 25–31. doi:10.1016/j.surfcoat.2018.08.061.

[46] Q.B. Nguyen, Z. Zhu, B.W. Chua, W. Zhou, J. Wei, S.M.L. Nai, Development of WC-Inconel composites using selective laser melting, Arch. Civ. Mech. Eng. 18 (2018) 1410–1420. doi:10.1016/j.acme.2018.05.001.

[47] C. Hong, D. Gu, D. Dai, M. Alkhayat, W. Urban, P. Yuan, S. Cao, A. Gasser, A. Weisheit, I. Kelbassa, M. Zhong, R. Poprawe, Laser additive manufacturing of ultrafine TiC particle reinforced Inconel 625 based composite parts: Tailored microstructures and enhanced performance, Mater. Sci. Eng. A. 635 (2015) 118–128. doi:10.1016/j.msea.2015.03.043.

[48] T.E. Abioye, P.K. Farayibi, D.G. McCartney, A.T. Clare, Effect of carbide dissolution on the corrosion performance of tungsten carbide reinforced Inconel 625 wire laser coating, J. Mater. Process. Technol. 231 (2016) 89–99. doi:10.1016/j.jmatprotec.2015.12.023.

[49] D. Verdi, M.A. Garrido, C.J. Múnez, P. Poza, Mechanical properties of Inconel 625 laser cladded coatings: Depth sensing indentation analysis, Mater. Sci. Eng. A. 598 (2014) 15–21. doi:10.1016/j.msea.2014.01.026.

[50] X. Xu, G. Mi, L. Xiong, P. Jiang, X. Shao, C. Wang, Morphologies, microstructures and properties of TiC particle reinforced Inconel 625 coatings obtained by laser cladding with wire, J. Alloys Compd. 740 (2018) 16–27. doi:10.1016/j.jallcom.2017.12.298.

[51] M.Y. Shen, X.J. Tian, D. Liu, H.B. Tang, X. Cheng, Microstructure and fracture behavior of TiC particles reinforced Inconel 625 composites prepared by laser additive manufacturing, J. Alloys Compd. 734 (2018) 188–195. doi:10.1016/j.jallcom.2017.10.280.

[52] T.E. Abioye, D.G. Mccartney, A.T. Clare, Journal of Materials Processing Technology Laser cladding of Inconel 625 wire for corrosion protection, J. Mater. Process. Tech. 217 (2015) 232–240. doi:10.1016/j.jmatprotec.2014.10.024.

[53] D. Verdi, M.A. Garrido, C.J. Múnez, P. Poza, Microscale effect of high-temperature exposition on laser cladded Inconel 625-Cr3C2metal matrix composite, J. Alloys Compd. 695 (2017) 2696–2705. doi:10.1016/j.jallcom.2016.11.185.

[54] D. Verdi, M.A. Garrido, C.J. Múnez, P. Poza, Cr 3 C 2 incorporation into an Inconel 625 laser cladded coating : Effects on matrix microstructure , mechanical properties and local scratch resistance, J. Mater. 67 (2015) 20–27. doi:10.1016/j.matdes.2014.10.086.

[55] T.E. Abioye, J. Folkes, D.G. McCartney, a T. Clare, Concurrent Inconel 625 wire and WC powder laser cladding on AISI 304 stainless steel, 37th Int. MATADOR 2012 Conf. 0 (2013) 355–359. doi:10.1179/1743294412Y.0000000073.

[56] D. Verdi, M.A. Garrido, C.J. Múnez, P. Poza, Microscale evaluation of laser cladded Inconel 625 exposed at high temperature in air, JMADE. 114 (2017) 326–338. doi:10.1016/j.matdes.2016.11.014.